Journal of Power Sources 249 (2014) 515–519

Contents lists available at ScienceDirect

Journal of Power Sources

journal homepage: www.elsevier.com/locate/jpowsour

Short communication

Photo-excitation promoted quality factor of carbon nanotubes

Yu-Hsien Lin, Yih-Farn Kao, Hsin-Jung Tsai, Wen-Kuang Hsu*

Department of Materials Science and Engineering, National TsingHua University, Hsinchu 30013, Taiwan

HIGHLIGHTS

- Carbon nanotubes exhibit *RCL* characteristics in an ac field.
- Quality factor of carbon nanotubes-made devices is measured to be as high as 10^4.
- Quality factor of carbon nanotubes can be further promoted by photo-excitation.

ARTICLE INFO

Article history:
Received 5 June 2013
Received in revised form
31 July 2013
Accepted 15 August 2013
Available online 29 August 2013

Keywords:
Carbon nanotubes
Quality factor
Photo-excitation
Electrical percolation

ABSTRACT

Carbon nanotubes exhibit characteristics of resistor–capacitor–inductor in alternating current field and quality factor is estimated to be as high as 1×10^4. This value can be optically promoted and improvement is verified as a result of photocurrent creation in tubes. Experimental data is supported by *ab-initio* calculations.

1. Introduction

The quality factor (Q) is a dimensionless parameter often used to characterize damping magnitude of an oscillating system and normally lies on 10^2–10^3 for alternating current (ac) driven electronics [1]. Impedance (Z) however emerges as current (I) and voltage (V) oscillate and is expressed as

$$Z = R - j/\omega C + j\omega L \tag{1}$$

where R is resistance, j is imaginary number, ω is angular frequency, C is capacitance and L is inductance; the 2nd and 3rd terms correspond to capacitive (X_C) and inductive reactance (X_L). For resistive circuits, sine wave amplitudes of I and V are always in-phase and imaginary part of Z is zero (i.e. $-j/\omega C = 0$, $j\omega L = 0$) [1–4]. Phase difference occurs as device contains reactive components (i.e. capacitor & inductor) and reactance begins to contribute to Z (i.e. $-j/\omega C + j\omega L \neq 0$). At resonant frequency (ω_o), X_C and X_L cancel each other (i.e. $-j/\omega C + j\omega L = 0$) and energy storage at capacitor and inductor reaches a maximum. In this case, input power is multiplied by Q expressed as

$$Q = \frac{L\omega_0}{R} = \frac{1}{CR\omega_0} = \frac{1}{R}\sqrt{\frac{L}{C}} \tag{2}$$

Carbon nanotubes (CNTs) are one dimension conductor made of rounded graphene sheets and do not suffer from the peierls distortion at low temperature [5]. Electrical measurements reveal that CNTs also behave as reactive elements in ac field (Fig. 1) and damping originates from curvature induced dipole relaxation and chiral current [6,7]. At low $\omega < 1000$ Hz, Z is mainly contributed by R and both X_C and X_L approximate zero. Spins become polarized as ω increases and X_C begins to contribute to Z. Calculation reveals $X_C = 40$–$50\ \Omega$ and X_L due to circulating current lies on 0.1–1 Ω [8–16]. Studies however lack explanation on energy loss mechanism and Q remains unexplored. In this work, devices that contain a low content of CNTs are made and Q is measured at dark (Q_{off}) and bright conditions (Q_{on}). We find $Q_{on}/Q_{off} > 1$ and both Q_{off} and Q_{on} reach a level comparable with that on oxide-based resonators. Optical enhancement has been identified as a result of photocurrent (I_{photo}) creation in nanotubes and is supported by $I_{photo} \propto Q_{on}/Q_{off}$. Photo-carriers however tend to couple with leads; thus create interfacial

* Corresponding author. Tel.: +886 3 5715131x35399.
E-mail address: wkhsu@mx.nthu.edu.tw (W.-K. Hsu).

0378-7753/$ – see front matter © 2013 Elsevier B.V. All rights reserved.
http://dx.doi.org/10.1016/j.jpowsour.2013.08.050

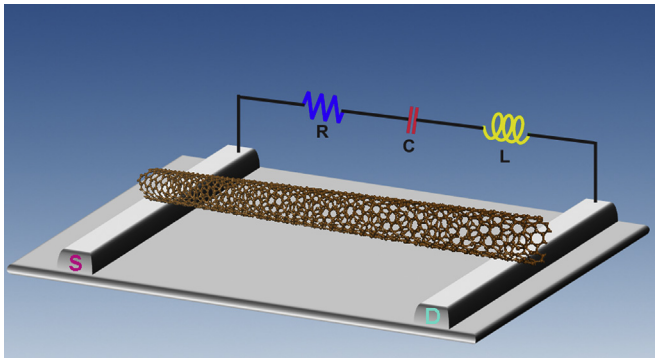

Fig. 1. Scheme of a CNT created *RCL* circuit.

reactance. Study reveals that I_{photo} also dissipates at tube boundaries and loss mechanism involves Schottky potential (E_{SCH}) induced hopping at metallic (M)/semiconducting (S) tube junctions.

2. Experimental

Arc-discharge produced single-walled CNTs (SWCNTs, 50 mg) are dispersed in H_2O_2/H_2O solution (1:1 weight %, 100 ml) and oxidation is carried out at 50 °C for 2 h. Oxidized CNTs are deposited onto SiO_2 substrate supported Al electrodes and devices are then placed in a vacuum chamber (10^{-5} torr) equipped with electrical fit-through and laser pointer (632 nm wavelength, spot size 0.5 ~ 1 mm, 5 mW, Horiba-HR800). Compared with single tube, CNT networks produce a large I_{photo} and therefore promote accuracy of electrical measurements [5,8]. The R and I_{photo} are probed with a network analyser (Zentech-3302, ac mode, ω = 0.1 KHz–1 MHz, background noise = ±0.5 nA) and measurements are carried out at various temperatures (T) and bias voltages (V_{bias}). The Q is determined according criteria given by Eq. (2); (i) the R minimum and I maximum (I_{max}) emerge at ω_o; (ii) $I \geq 0.707 I_{max}$ takes place at pass-band width of frequency ($\Delta\omega$) [Fig. 2(a)] [1]; (iii) R is inversely proportional to Q (i.e. $R \propto Q^{-1}$). We first scan devices from 0.1 KHz to 1 MHz to monitor I variation and $\Delta\omega$ is determined by $I \geq 0.707 I_{max}$. Once $\Delta\omega$ is located the input I is switched from course (mA–μA) to fine (μA–nA) modulation to spot I_{max} and ω_o [Fig. 2(a)]. It is worth mentioning that both SWCNTs and Al-electrodes have a similar work function (4.25–4.28 eV) and do not form an E_{SCH} capable of producing I_{photo} at interfaces [12].

3. Results and discussion

Fig. 2(b) shows R–ω profiles obtained from three different samples and ω_o (i.e. R minimum) appears at 170 ± 20 KHz for sample-1, 168 ± 17 KHz for sample-2 and 166 ± 18 KHz for sample-3; the ω_o variation from sample to sample being the fact that tubes are arranged in various configurations between leads [1,2]. Q however does not change with tube arrangements and is determined only by Z [17]. Fig. 3(a) shows Q–ω profiles of sample-1 at T = 300 K and, the Q_{off} and Q_{on} are calculated according to R profiles at light-off (R_{off}) and -on (R_{on}) [e.g. Fig. 2(b)]. It is clearly that Q_{on} exceeds Q_{off} and Q_{on}/Q_{off} approximates 2.1: both Q_{on} and Q_{off} are comparable with that on oxide-based resonators (~10^4) [2,3]. The $Q_{on} > Q_{off}$, according to Eq. (2), also means an enhanced energy storage at capacitor and inductor (i.e. increased C and L), accounting for ω_o shift from 181.4 KHz to 176.8 KHz [$\omega_o = 1/(LC)^{1/2}$, Fig. 3(a)]. Apparently, enhanced C and L originate from I_{photo} creation in CNTs and photo-excitation is further supported by $V_{bias} \propto I_{photo}$ [Fig. 3(b)] [18]. Fig. 4(a) and (b) plots C and L at light-off and -on and I_{photo} induced increase is estimated to be 3% and 1.5% for sample-1 (top), consistent with Fig. 3(a). Experiments carried out on sample

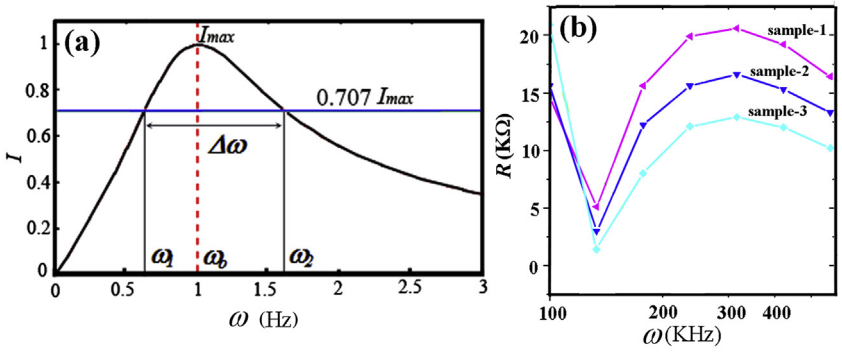

Fig. 2. (a) The relationship of I_{max} with $\Delta\omega$ and ω, (b) and R–ω plots.

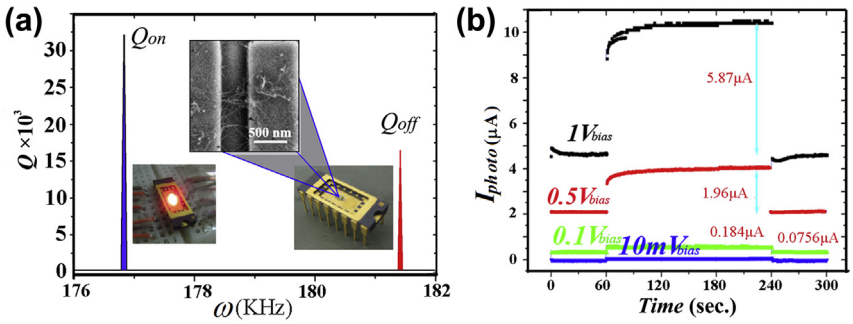

Fig. 3. (a) The Q–ω profile obtained from sample-1. Insets: SEM image of networked SWCNTs between leads (top), and device at illumination-off (right) and -on states (left). (b) The time evolved I_{photo} profiles of sample-1 at various V_{bias}.

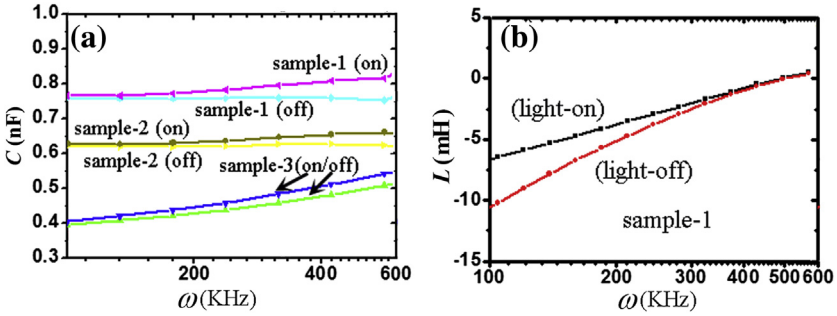

Fig. 4. (a) The C–ω plots obtained from sample 1–3 at illumination-off and -on states, and (b) L–ω plots of sample-1 at illumination-off and -on states.

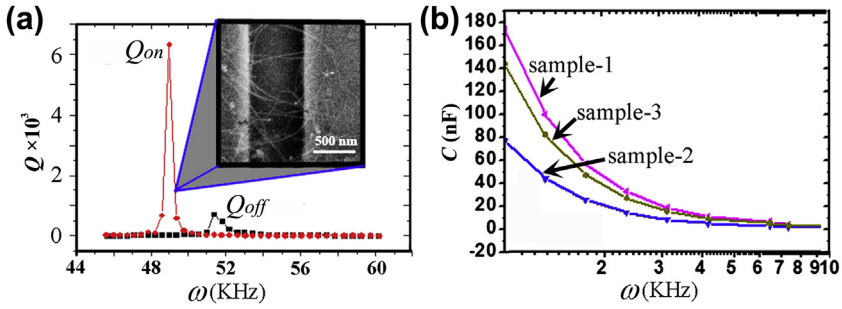

Fig. 5. (a) The Q–ω profile obtained from type-1. Inset: Enhanced SEM image of networked SWCNTs after repeated incidences by laser beam. (b) The C profiles at low ω.

Table 1
Electrical parameters at dark and bright conditions.

	Type 1		Type 2	
	Light-off	Light-on	Light-off	Light-on
ω_o (KHz)	51–55	49–52	152–155	148–151
R (KΩ)	0.104 ± 0.005	0.012 ± 0.001	0.9 ± 0.1	0.76 ± 0.05
Q_{on}/Q_{off}	8		1.2	
R_{off}/R_{on}	8		1.2	

2–3 give $O_{on}/Q_{off} = 8$ [Fig. 5(a)] and ω_o shift, according to Fig. 4(a) and (b), ranges at 3–5 Hz.

Over 20 samples have been measured and obtained data exhibits a relation of $Q_{on}/Q_{off} \propto R_{off}^{-1}$. For example, devices with low R_{off} give $Q_{on}/Q_{off} > 8$ (Type 1, Table 1) and $1 < Q_{on}/Q_{off} < 2$ emerges as R_{off} is large (Type 2, Table 1); the latter however implies a significant dissipation of I_{photo}. According to the electrical percolation model the equivalent circuit elements of current devices can be expressed as $R_{off} = \Sigma R_n + \Sigma 1/R_n + R_{con}$ where ΣR_n and $\Sigma 1/R_n$ represent nanotube resistors connected in series and parallel respectively and change as tubes are damaged [15]. SEM examination shows that CNTs remain intact after repeated incidences of laser and tube segmentation is absent, indicative of unchanged ΣR_n and $\Sigma 1/R_n$ [inset, Fig. 5(a)]. R_{con} is R arising from tube/lead contacts and controls transmission probability of CNTs [15]. In other words, R_{off} is dominated by R_{con} and equation can be rewritten as $Q_{on}/Q_{off} \propto R_{con}^{-1}$, i.e. the lower the R_{con} the greater the optical gain. Fig. 5(b) verifies R_{con} induced polarization [5] and C at $\omega < 2$ KHz reaches a value as high as 180 nF, corresponding to $X_C = 0.36$ Ω. Interfacial dissipation is further supported by observations that lighting induces a larger R decrease at reduced T and experiments give 15% at 5 K and 10% at 50 K with respect to Fig. 3(b), indicative of thermalization at tube/lead contacts [Fig. 6(a) and (b)] [17]. Similar results are also observed in 550 nm and 1100 nm excitations and Q_{off}/Q_{on} is measured to be 10.2 and 8.9 at 5 K and, 9.7 and 8.6 at 50 K [Fig. 6(a) and (b)].

Figs 5(b) and 6 clearly indicate that I_{photo} dissipates at tube/lead contacts [Fig. 7(a)] and reduced optical gain accounts for $1 < Q_{on}/$

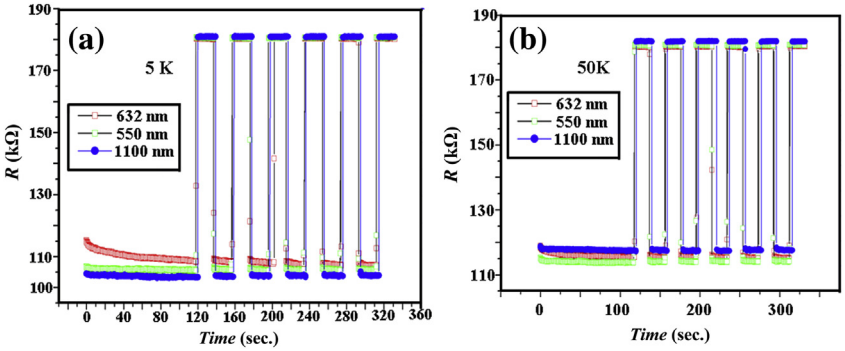

Fig. 6. (a) Time evolved R changes with photo-excitation by various wavelengths at 5 K and (b) 50 K.

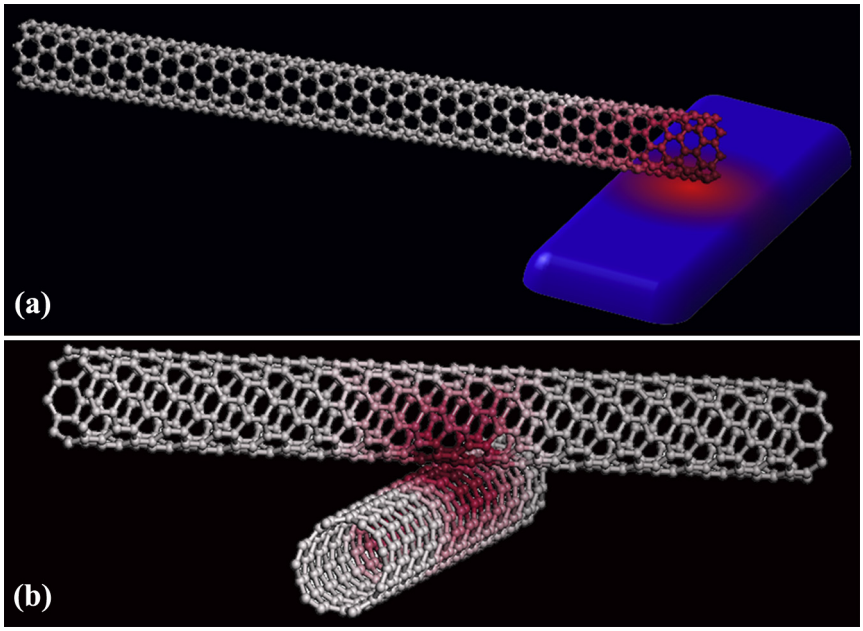

Fig. 7. I_{photo} dissipation at (a) tube-lead contact and (b) intertube junction.

$Q_{off} < 2$ (Type 2, Table 1). For aggregated tubes, excitonic relaxation also takes place at intertube junctions and phenomenon is owing to I_{photo} leakage through surface states, including dipolar lattices and dangling edges [18]. Study reveals that low energy channels are also present in M/S tube junctions [Fig. 7(b)] and E_{SCH} induced hopping is supported by *ab-initio* calculation below. First, S(10,0) and M(9,0) tubes are built in a $1 \times 1 \times 1$ nm cell and tube length is set as 21 nm.

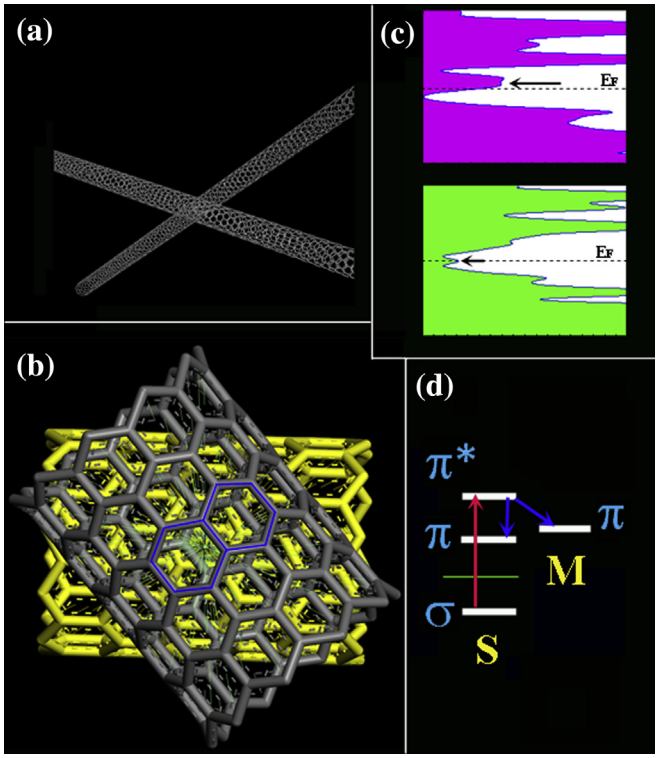

Fig. 8. (a) Simulated structure of crisscross tubes, (b) the nearest lattices with $E_{SCH} \neq 0$ (blue), (c) band diagrams of M- (top) and S-tube (lower) near to the E_F and (d) optical transition from π^*(S) to π(M).

Second, tubes are arranged in a crisscross fashion and three different combinations are computed, including S(10,0)/S(10,0), S(10,0)/M(9,0) and M(9,0)/M(9,0) [Fig. 8(a) and (b)]. Third, structures are geometrically optimized and intertube potential is converged to the van der Waal's regime [18,19]. Fourth, the band diagram is calculated according to density functional theory and charge density is measured with a standard *k*-point path method [20,21]. Calculation reveals that tubes interact through electronic states near to Fermi level (E_F) [arrows, Fig. 8(c)] and E_{SCH} at S/S and M/M interfaces approaches zero. Transfer however takes place at M/S tube junction and E_{SCH} is calculated to be 3.4 kcal mol^{-1}, corresponding to 1 eV [22]. Fig. 8(d) shows a possible scenario for intertube transfer: first, excitons are created at π^* state (S-tube) and becomes free carriers at $V_{bias} \neq 0$; second, intertube transition of π^*(S-tube) $\rightarrow$ π(M-tube) occurs and incommensurate alignment of wave vector at E_F causes carrier scattering at M-tube surfaces. The $\pi^*(S) \rightarrow \pi(M)$ transition is supported by changeover from negative to positive temperature coefficient of resistivity previously observed in a similar experiment [18]. Yoon et al. have studied the conductance of CNTs at compressive status and data reveal that tunneling proceeds preferentially at deformed lattices. Conductance then drops by two orders of magnitude as load is removed and hopping takes place only at correlated lattices [20]. Crisscrossed tubes, however, cannot electronically correlate and hopping occurs only at the nearest lattices with $E_{SCH} \neq 0$, corresponding to a naphthalene [blue, Fig. 8(b)].

4. Conclusion

SWCNTs exhibit *RCL* characteristics in ac field and *Q* is measured to be as high as 1×10^4. This value can be optically promoted and improvement originates from enhanced *C* and *L* upon I_{photo} creation in CNTs. Surface losses account for $1 < Q_{on}/Q_{off} < 2$ I_{photo} and I_{photo} dissipates at tube/lead contacts and S/M tube junctions.

Acknowledgment

We thank the National Science Council of Taiwan for the financial support (NSC-101-2112-M-007-011-MY2).

References

[1] S. Pipilos, Y.P. Tsividis, J. Fenk, Y. Papananos, IEEE J. Solid-State Circuits 31 (1996) 1517–1525.
[2] V.B. Braginsky, M.L. Gorodetsky, V.S. Ilchenko, Phys. Lett. A 137 (1989) 393–397.
[3] T. Baehr-Jones, M. Hochberg, C. Walker, A. Scherer, Appl. Phys. Lett. 86 (2005) 081101–081103.
[4] M. Gustafsson, S. Nordebo, Prog. Electromagn. Res. 62 (2006) 1–20.
[5] C.L. Kane, E.J. Mele, Phys. Rev. Lett. 78 (1997) 1932–1935.
[6] Y.C. Su, W.K. Hsu, Appl. Phys. Lett. 87 (2005).
[7] A. Star, Y. Lu, K. Bradley, G. Grüner, Nano Lett. 4 (2004) 1587–1591.
[8] R. Martel, T. Schmidt, H.R. Shea, T. Hertel, P. Avouris, Appl. Phys. Lett. 73 (1998) 2447–2449.
[9] C. Dekker, Phys. Today 52 (1999) 22–28.
[10] P.G. Collins, K. Bradley, M. Ishigami, A. Zettl, Science 287 (2000) 1801–1804.
[11] J. Kong, N.R. Franklin, C. Zhou, M.G. Chapline, S. Peng, K. Cho, H. Dai, Science 287 (2000) 622–625.
[12] D.H. Lien, W.K. Hsu, H.W. Zan, N.H. Tai, C.H. Tsai, Adv. Mater. 18 (2006) 98–103.
[13] Y.P. Zhao, B.Q. Wei, P.M. Ajayan, G. Ramanath, T.M. Lu, G.C. Wang, A. Rubio, S. Roche, Phys. Rev. B 64 (2001).
[14] W.G. Zhu, E. Kaxiras, Appl. Phys. Lett. 89 (2006).
[15] W.K. Hsu, V. Kotzeva, P.C.P. Watts, G.Z. Chen, Carbon 42 (2004) 1707–1712.
[16] P.C.P. Watts, W.K. Hsu, Appl. Phys. A 78 (2004) 79–83.
[17] C.P. Yue, S.S. Wong, IEEE J. Solid-State Circuits 33 (1998) 743–752.
[18] Y.H. Lin, Y.C. Lai, C.T. Hsu, C.J. Hu, W.K. Hsu, Phys. Chem. Chem. Phys. 13 (2011) 7118–7122.
[19] H.C. Li, S.Y. Lu, S.H. Syue, W.K. Hsu, S.C. Chang, Appl. Phys. Lett. 93 (2008).
[20] Y.G. Yoon, M.S.C. Mazzoni, H.J. Choi, J. Ihm, S.G. Louie, Phys. Rev. Lett. 86 (2001) 688–691.
[21] S.H. Syue, C.T. Hsu, U.S. Chen, H.J. Chen, W.K. Hsu, H.C. Shih, Carbon 47 (2009) 1239–1243.
[22] S.K. Lee, C.M. Zetterling, M. Ostling, J. Electron. Mater. 30 (2001) 242–246.